LBL-11171 c.2
Preprint

Lawrence Berkeley Laboratory
UNIVERSITY OF CALIFORNIA

Submitted to Nuclear Physics A

THE TWO-LEVEL MODEL AT FINITE-TEMPERATURE

Alan L. Goodman

July 1980

TWO-WEEK LOAN COPY

This is a Library Circulating Copy which may be borrowed for two weeks. For a personal retention copy, call Tech. Info. Division, Ext. 6782

NUCLEAR SCIENCE DIVISION

Prepared for the U.S. Department of Energy under Contract W-7405-ENG-48

LBL-11171 c.2

LBL-11171

THE TWO-LEVEL MODEL AT FINITE-TEMPERATURE

Alan L. Goodman*

Physics Department and Quantum Theory Group
Tulane University
New Orleans, Louisiana 70118†

and

Nuclear Science Division
Lawrence Berkeley Laboratory
University of California
Berkeley, California 94720

ABSTRACT

The finite-temperature HFB cranking equations are solved for the two-level model. The pair gap, moment-of-inertia and internal energy are determined as functions of spin and temperature. Thermal excitations and rotations collaborate to destroy the pair correlations. Raising the temperature eliminates the backbending effect and improves the HFB approximation.

*Supported in part by the National Science Foundation.
†Present address.

1. INTRODUCTION

Hartree-Fock-Bogoliubov (HFB) calculations have been primarily restricted to the yrast line, which consists of the lowest energy state for each spin.[1] However, heavy-ion reactions populate regions above the yrast line which contain a high density of nuclear states. The average properties of these states may be described by introducing a temperature T. The yrast line corresponds to $T = 0$. Figure 1 illustrates how the excitation energy of a nucleus can be split into thermal and collective components.

The finite-temperature HFB cranking (FTHFBC) equations have been derived in a separate article.[2] This theory provides a framework for investigating nuclear properties above the yrast line. For a first attempt to solve the FTHFBC equations, it seems advisable to choose a simple model Hamiltonian rather than embark upon more realistic calculations. The model selected is the two-level model of Krumlinde and Szymanski.[3] The HFBC treatment of this model at zero-temperature has been extensively studied,[3-8] so it is appropriate to extend prior investigations to finite-temperature. The model contains a single-particle splitting, a pairing force, an angular momentum operator which induces rotations, and a finite-temperature is introduced. (The rotor is omitted here.) So although the model is quite simple, it contains several essential features of real nuclei. Finite-temperature and rotations each destroy pair correlations. This model illustrates in a self-consistent fashion the inter-dependence of thermal excitations, rotations, and pairing.

2. REVIEW OF FINITE-TEMPERATURE HFB CRANKING THEORY

The FTHFB equations are[2]

$$\begin{pmatrix} \mathcal{H} & \Delta \\ -\Delta^* & -\mathcal{H}^* \end{pmatrix} \begin{pmatrix} U_i \\ V_i \end{pmatrix} = E_i \begin{pmatrix} U_i \\ V_i \end{pmatrix} \quad , \tag{2.1}$$

where U_i is the vector $(U_{i1}, U_{i2}, \ldots)$ and E_i is the energy of the quasiparticle

$$a_i^\dagger = \sum_j (U_{ij} C_j^\dagger + V_{ij} C_j) \quad . \tag{2.2}$$

The HF Hamiltonian $\mathcal{H}$, the HF potential Γ, and the pair potential Δ are

$$\mathcal{H}_{ij} = (T - \mu - \omega J_x + \Gamma)_{ij} \quad , \tag{2.3}$$

$$\Gamma_{ij} = \sum_{k\ell} \langle ik|v_a|j\ell \rangle \rho_{\ell k} \quad , \tag{2.4}$$

$$\Delta_{ij} = \tfrac{1}{2} \sum_{k\ell} \langle ij|v_a|k\ell \rangle t_{k\ell} \quad . \tag{2.5}$$

The density matrix ρ and the pairing tensor t are

$$\rho_{ij} = \langle C_j^\dagger C_i \rangle = [\tilde{U} f U^* + V^\dagger (1-f) V]_{ij} \quad , \tag{2.6}$$

$$t_{ij} = \langle C_j C_i \rangle = [\tilde{U} f V^* + V^\dagger (1-f) U]_{ij} \quad . \tag{2.7}$$

The quasiparticle occupation probability f is

$$f_{ij} = f_i \delta_{ij} \quad , \qquad f_i = \frac{1}{1 + e^{\beta E_i}} \quad , \tag{2.8}$$

where $\beta = 1/kT$, k is Boltzmann's constant, and T is the temperature. The chemical potential μ and the angular velocity ω are adjusted to

satisfy the number and spin constraints

$$\langle \hat{N} \rangle = N \quad , \tag{2.9}$$

$$\langle J_x \rangle = [J(J+1)]^{\frac{1}{2}} \equiv I \quad . \tag{2.10}$$

The internal energy is

$$E = \langle H \rangle = \mathrm{Tr}[(T + \tfrac{1}{2}\Gamma)\rho + \tfrac{1}{2}\Delta t^{\dagger}] \quad , \tag{2.11}$$

and the entropy is

$$S = -k \sum_i [f_i \ln f_i + (1-f_i) \ln (1-f_i)] \ . \tag{2.12}$$

The grand potential in a rotating frame is

$$\Omega = E - TS - \mu N - \omega I \quad . \tag{2.13}$$

The FTHFBC equations (2.1) are derived from the variational principle

$$\delta\Omega = 0 \quad , \tag{2.14}$$

and the independent quasiparticle approximation

$$H \approx H_{HFB} = E_o + \sum_i E_i a_i^{\dagger} a_i \quad . \tag{2.15}$$

3. TWO-LEVEL MODEL

The two-level model contains Ω identical sets of four states. One of these sets is shown in Fig. 2. The levels are half-filled so that $N = 2\Omega$ and the chemical potential $\mu = 0$. The rotor is omitted. The Hamiltonian is

$$H = H_{s.p.} + H_p \quad , \tag{3.1}$$

where the single-particle and pair components are

$$H_{s.p.} = \varepsilon \sum_{i=1}^{\Omega} (c_{1i}^{\dagger}c_{1i} + c_{3i}^{\dagger}c_{3i} - c_{2i}^{\dagger}c_{2i} - c_{4i}^{\dagger}c_{4i}) \quad , \tag{3.2}$$

$$H_p = -G \sum_{i,j=1}^{\Omega} (c_{1i}^{\dagger}c_{3i}^{\dagger} + c_{2i}^{\dagger}c_{4i}^{\dagger})(c_{3j}c_{1j} + c_{4j}c_{2j}) \quad , \tag{3.3}$$

The motion is restricted to two dimensions and the angular momentum is

$$J_x = \tfrac{1}{2} \sum_{i=1}^{\Omega} (c_{1i}^{\dagger}c_{2i} - c_{3i}^{\dagger}c_{4i} + h.c.) \quad , \tag{3.4}$$

where each particle has $J_x = \pm\frac{1}{2}$ and the maximum spin is $\langle J_x \rangle = \Omega$. When $T = 0$, the exact energies of this system are given by the R(5) model of Krumlinde and Szymanski.[3]

For this model the HF Hamiltonian and the pair potential are block diagonal in the index i, which specifies one of the Ω sets of four levels shown in Fig. 2. Consequently the FTHFBC equation (2.1) reduces to Ω identical 8×8 blocks. The index i will now be omitted. The matrices below are represented in the basis 1,2,3,4 of Fig. 2.

The angular momentum operator is

$$J_x = \begin{bmatrix} 0 & \frac{1}{2} & 0 & 0 \\ \frac{1}{2} & 0 & 0 & 0 \\ 0 & 0 & 0 & -\frac{1}{2} \\ 0 & 0 & -\frac{1}{2} & 0 \end{bmatrix} \quad . \tag{3.5}$$

The contribution of the pair interaction to the HF potential (2.4) is neglected, so that $\Gamma = 0$. The HF Hamiltonian (2.3) is

$$\mathcal{H} = \begin{bmatrix} \varepsilon & -\omega/2 & 0 & 0 \\ -\omega/2 & -\varepsilon & 0 & 0 \\ 0 & 0 & \varepsilon & \omega/2 \\ 0 & 0 & \omega/2 & -\varepsilon \end{bmatrix} , \tag{3.6}$$

and the pair potential (2.5) is

$$\Delta = \begin{bmatrix} 0 & 0 & -\Delta & 0 \\ 0 & 0 & 0 & -\Delta \\ \Delta & 0 & 0 & 0 \\ 0 & \Delta & 0 & 0 \end{bmatrix} , \tag{3.7}$$

where

$$\Delta = G\Omega(t_{13} + t_{24}) \quad . \tag{3.8}$$

The eigenvalues E_i of Eq. (2.1) are the quasiparticle energies[4]

$$E_1 = E_3 = E_+ \quad , \quad E_2 = E_4 = E_- \quad , \tag{3.9}$$

where

$$E_\pm = [\varepsilon^2 + (\Delta \pm \omega/2)^2]^{\frac{1}{2}} \quad , \tag{3.10}$$

and the eigenvectors of Eq. (2.1) define the quasiparticle transformations (2.2),[5]

$$U = \begin{bmatrix} A_+ & -B_+ & 0 & 0 \\ A_- & B_- & 0 & 0 \\ 0 & 0 & A_+ & B_+ \\ 0 & 0 & A_- & -B_- \end{bmatrix} , \tag{3.11}$$

$$V = \begin{bmatrix} 0 & 0 & -B_+ & A_+ \\ 0 & 0 & -B_- & -A_- \\ B_+ & A_+ & 0 & 0 \\ B_- & -A_- & 0 & 0 \end{bmatrix} , \tag{3.12}$$

where

$$A_\pm = \tfrac{1}{2}[1 + \varepsilon/E_\pm]^{\frac{1}{2}} , \tag{3.13}$$

$$|B_\pm| = \tfrac{1}{2}[1 - \varepsilon/E_\pm]^{\frac{1}{2}} , \tag{3.14}$$

and $A_\pm$ and B_+ are positive, whereas B_- is positive when $\Delta > \omega/2$ and negative when $\Delta < \omega/2$. The spin is

$$\langle J_x \rangle = \mathrm{Tr}(\rho J_x) = \Omega(\rho_{12} - \rho_{34}) , \tag{3.15}$$

the moment-of-inertia is

$$\mathscr{I} = \langle J_x \rangle/\omega , \tag{3.16}$$

and the internal energy (2.11) is

$$E = \Omega\varepsilon(\rho_{11} + \rho_{33} - \rho_{22} - \rho_{44}) - \Delta^2/G . \tag{3.17}$$

The essential difference between the finite-temperature and zero-temperature cases is that the quasiparticles have a non-zero occupation probability (2.8) when $T \neq 0$

$$f = \begin{bmatrix} f_+ & 0 & 0 & 0 \\ 0 & f_- & 0 & 0 \\ 0 & 0 & f_+ & 0 \\ 0 & 0 & 0 & f_- \end{bmatrix} , \tag{3.18}$$

where

$$f_{\pm} = \frac{1}{1 + e^{\beta E_{\pm}}} \quad . \tag{3.19}$$

The density matrix ρ is evaluated by substituting Eqs. (3.11), (3.12) and (3.18) into Eq. (2.6),

$$\rho = \begin{bmatrix} \rho_{11} & \rho_{12} & 0 & 0 \\ \rho_{12} & \rho_{22} & 0 & 0 \\ 0 & 0 & \rho_{11} & -\rho_{12} \\ 0 & 0 & -\rho_{12} & \rho_{22} \end{bmatrix} \quad , \tag{3.20}$$

where

$$\rho_{11} = \frac{1}{2} - \frac{\varepsilon}{4} \left[\frac{\tanh(\frac{1}{2}\beta E_+)}{E_+} + \frac{\tanh(\frac{1}{2}\beta E_-)}{E_-} \right] \quad , \tag{3.21}$$

$$\rho_{22} = \frac{1}{2} + \frac{\varepsilon}{4} \left[\frac{\tanh(\frac{1}{2}\beta E_+)}{E_+} + \frac{\tanh(\frac{1}{2}\beta E_-)}{E_-} \right] \quad , \tag{3.22}$$

$$\rho_{12} = \frac{1}{4} \left[\frac{(\Delta + \omega/2)}{E_+} \tanh(\tfrac{1}{2}\beta E_+) - \frac{(\Delta - \omega/2)}{E_-} \tanh(\tfrac{1}{2}\beta E_-) \right] \quad . \tag{3.23}$$

Similarly the pairing tensor t of Eq. (2.7) is

$$t = \begin{bmatrix} 0 & 0 & t_{13} & -t_{23} \\ 0 & 0 & t_{23} & t_{13} \\ -t_{13} & -t_{23} & 0 & 0 \\ t_{23} & -t_{13} & 0 & 0 \end{bmatrix} \quad , \tag{3.24}$$

where

$$t_{13} = \frac{1}{4} \left[\frac{(\Delta + \omega/2)}{E_+} \tanh(\tfrac{1}{2}\beta E_+) + \frac{(\Delta - \omega/2)}{E_-} \tanh(\tfrac{1}{2}\beta E_-) \right] \quad , \tag{3.25}$$

$$t_{23} = \frac{\varepsilon}{4}\left[\frac{\tanh(\frac{1}{2}\beta E_+)}{E_+} - \frac{\tanh(\frac{1}{2}\beta E_-)}{E_-}\right]. \tag{3.26}$$

When $T=0$ $(\beta=\infty)$, then $\tanh(\frac{1}{2}\beta E_\pm) = 1$.

The finite-temperature cranked gap equation is found by substituting Eq. (3.25) into Eq. (3.8),

$$\Delta = \frac{G\Omega}{2}\left[\frac{(\Delta + \omega/2)}{E_+}\tanh(\tfrac{1}{2}\beta E_+) + \frac{(\Delta - \omega/2)}{E_-}\tanh(\tfrac{1}{2}\beta E_-)\right] . \tag{3.27}$$

When the spin and temperature are zero, then

$$\Delta = [G^2\Omega^2 - \varepsilon^2]^{\frac{1}{2}} \quad , \qquad (\omega = T = 0) \quad . \tag{3.28}$$

The spin (3.15) is

$$I \equiv \langle J_x \rangle = \frac{\Omega}{2}\left[\frac{(\Delta + \omega/2)}{E_+}\tanh(\tfrac{1}{2}\beta E_+) - \frac{(\Delta - \omega/2)}{E_-}\tanh(\tfrac{1}{2}\beta E_-)\right] . \tag{3.29}$$

When $\omega=0$, then $E_+ = E_-$ and $\langle J_x \rangle = 0$. The internal energy (3.17) is

$$E = -\Omega\varepsilon^2\left[\frac{\tanh(\frac{1}{2}\beta E_+)}{E_+} + \frac{\tanh(\frac{1}{2}\beta E_-)}{E_-}\right] - \frac{\Delta^2}{G} \quad , \tag{3.30}$$

and the entropy (2.12) is

$$S = -2k\Omega \sum_{f=f_\pm} [f \ln f + (1-f)\ln(1-f)] \quad . \tag{3.31}$$

When $T=0$, then $S=0$.

For $\omega=0$, the critical temperature T_c at which Δ vanishes is

$$kT_c = \frac{\varepsilon}{2\tanh^{-1}(\varepsilon/G\Omega)} \quad , \qquad (\omega = 0) \quad . \tag{3.32}$$

In the degenerate model $(\varepsilon=0)$, Eq. (3.32) reduces to

$$kT_c = G\Omega/2 \quad , \qquad (\varepsilon = \omega = 0) \quad . \tag{3.33}$$

4. SOLUTION OF THE GAP EQUATION

The function $\Delta(\omega,T)$ is determined numerically by choosing values for ω and T, and searching for values of Δ which satisfy the finite-temperature gap equation (3.27). All other quantities are then directly evaluated.

The effect of raising the temperature in the non-rotating case ($\omega = 0$) is shown in Fig. 3. At the critical temperature given by Eq. (3.32) there is a "phase transition" from a pair correlated state to a normal state. The thermal excitations create a blocking effect which destroys the pairing.

The gap $\Delta(\omega)$ is given for various temperatures in Figs. 4 and 5. These figures illustrate how rotations and thermal excitations collaborate to break down the pair gap. For $kT < 0.3$ MeV, the curves are triple-valued, indicative of the "backbending" effect; whereas for $kT > 0.3$ MeV, there is no backbending.

The critical spin I_c is defined as the spin for which Δ goes to zero. Figure 6 shows I_c versus the temperature. As T increases, I_c decreases. When $T = T_c$, then I_c goes to zero.

The spin of Eq. (3.29) is given in Fig. 7. For small ω, increasing the temperature causes the spin to increase. This is the pairing region, and pairing resists rotation-alignment. However, raising T decreases Δ, which makes it easier for the spins to align. By contrast, at high values of ω, increasing the temperature causes the spin to decrease. At $T = 0$, the completely aligned state $I = \Omega$ is nearly produced. However, raising T creates thermal excitations out of the completely aligned state, which reduces the spin. It can be shown that each particle has the same spin,

which is therefore equal to $I/2\Omega$. The particles all align in exactly the same manner. The cusps near the top of each curve correspond to the point at which $\Delta \to 0$.

The moment-of-inertia (3.16) is shown in Fig. 8. At $T = 0$ there is a giant backbending. For intermediate temperature the backbending disappears. When $T > T_c$ the moment-of-inertia is nearly constant.

The internal energy (3.30) as a function of temperature is given in Fig. 9 for $I = 0,4,8$. The changes in the energies are primarily due to the collapse of the pair gap. The variations in the single-particle (HF) energy are very small. Since the pair gap at $T = 0$ decreases as I increases, it follows that the temperature dependence of the energy decreases as I increases.

The internal energy as a function of spin is shown in Fig. 10 for several temperatures. For $T = 0$ the yrast line is concave down, indicating a sharp backbending, whereas at $kT = 0.4$ MeV there is no backbending.

Once the internal energy $E(I,T)$ has been calculated, Fig. 1 indicates that it may be decomposed into ground state, collective, and thermal contributions,

$$E(I,T) = E_{gs} + E_{coll}(I) + E_{therm}(I,T) \quad , \tag{4.1}$$

where

$$E_{gs} = E(0,0) \quad , \tag{4.2}$$

$$E_{coll}(I) = E(I,0) - E(0,0) \quad , \tag{4.3}$$

$$E_{therm}(I,T) = E(I,T) - E(I,0) \quad . \tag{4.4}$$

These energies are given by Fig. 8 and Fig. 9.

The quasiparticle occupation probabilities of Eq. (3.19) are given in Fig. 11. For the model considered here, the quasiparticle energies (3.10) are non-negative, so that $0 \leqslant f_{\pm} \leqslant \frac{1}{2}$. In more realistic calculations the quasiparticle energies can become negative in the backbending region,[1] and then $0 \leqslant f_i \leqslant 1$. Consider the $I = 0$ curve. Then $\omega = 0$, so that $E_+ = E_-$ and $f_+ = f_-$. As T increases, Δ and E decrease, so that f increases. For $kT \geqslant kT_c = 0.498$ MeV, then $\Delta = 0$ and $E = \varepsilon = 0.1$ MeV $\ll kT$, so that $f \approx \frac{1}{2}$ for $T > T_c$. Next consider the $I = 4$ curves. At $kT \approx 0.35$ MeV, $\Delta = \omega/2$, so that E_- has a minimum and f_- has a maximum. For $kT > 0.35$ MeV, E_- increases more rapidly than kT, so that f_- decreases. At $kT \approx 0.45$ MeV, $\Delta = 0$ and $f_+ = f_-$ for higher temperatures. For $I = 8$, $\Delta = 0$ when $kT > 0.15$ MeV, and then $f_+ = f_-$.

Figure 11 shows that at high temperatures, f is independent of T and f decreases as I increases. The explanation is as follows: at high temperatures where $\Delta = 0$ and $\omega/2 \gg \varepsilon$, Eq. (3.29) reduces to

$$f_{\pm} \approx \tfrac{1}{2}(1 - I/\Omega) \quad . \tag{4.5}$$

Consequently f is independent of the temperature. Since $E \approx \omega/2$, it follows that ω is proportional to T when I is held constant. Equation (4.5) also shows that f decreases as the spin increases, and $f = 0$ when the spin acquires the maximum value of Ω.

The entropy (3.31) is depicted in Fig. 12. When $f_{\pm} = \frac{1}{2}$, then S is maximized, and

$$(S/k)_{max} = 4\Omega \ln 2 \quad . \tag{4.6}$$

For $\Omega = 10$, $(S/k)_{max} = 27.73$. The features of the entropy curves are dictated by the occupations $f_{\pm}$ of Fig. 11.

5. ANGULAR MOMENTUM FLUCTUATION ENERGY

An approximate angular momentum projection is achieved by correcting the FTHFBC energy by the angular momentum fluctuation energy[9,10]

$$E_{proj}(I,T) \approx E_{FTHFBC}(I,T) - E_{fluct}(I,T) \quad , \tag{5.1}$$

where

$$E_{fluct}(I,T) = (\Delta J_x)^2/2\mathcal{J}_{FTHFBC} \quad , \tag{5.2}$$

$\mathcal{J}_{FTHFBC}$ is given by Eq. (3.16), and E_{FTHFBC} is given by Eq. (3.30). If E_{fluct} is independent of I, then FTHFBC gives the correct values for E_{coll}. Similarly if E_{fluct} is independent of T, then FTHFBC gives the correct values for E_{therm}. Consequently if E_{fluct} is independent of I (T), then the energy of a transition at constant T (I) is correctly given by FTHFBC.

The square of the fluctuation in J_x is[10]

$$(\Delta J_x)^2 = \mathrm{Tr}[J_x^2\rho - (J_x\rho)^2 - J_x t\, J_x^* t^*] \quad , \tag{5.3}$$

where J_x, ρ and t are given by Eqs. (3.5), (3.20), and (3.24). The result is

$$(\Delta J_x)^2 = \frac{\Omega}{4}\left[1 - \left(\frac{I}{\Omega}\right)^2 - \left(\frac{\Delta}{G\Omega}\right)^2 + \frac{1}{2}\left(\frac{\varepsilon \tanh(\frac{1}{2}\beta E_+)}{E_+}\right)^2 + \frac{1}{2}\left(\frac{\varepsilon \tanh(\frac{1}{2}\beta E_-)}{E_-}\right)^2\right] , \tag{5.4}$$

where $I_{max} = \Omega$ and $\Delta_{max} = G\Omega$.

The fluctuation in J_x is shown in Fig. 13 and the fluctuation energy is given in Fig. 14. Observe that increasing the temperature reduces the spin dependence of the fluctuation energy, and increasing the spin reduces the temperature dependence of the fluctuation energy. This indicates that

the HFB approximation improves as the temperature or spin increases. Comparing Figs. 10 and 14, observe that the fluctuation energy is smaller than the FTHFBC energy by a factor of 13 at $kT = 0$ and 41 at $kT = 0.3$ MeV.

6. CONCLUSIONS

The FTHFBC theory is used to derive the finite-temperature cranked gap equation for the two-level model. Solution of the gap equation provides various nuclear properties as functions of spin and temperature. The manner in which rotations and thermal excitations mutually conspire to destroy the pair gap is illustrated. For this model, increasing the temperature eliminates the backbending and improves the HFB approximation.

Acknowledgments

The author is indebted to R. Diamond for a hospitable visit to Lawrence Berkeley Laboratory.

Part of this work was done under the auspices of the Nuclear Physics Division of the U.S. Department of Energy under contract W-7405-ENG-48.

REFERENCES

1. A.L.Goodman, in Advances in Nuclear Physics, ed. J.Negele and E.Vogt, Vol. 11 (Plenum Press, New York, 1979).
2. A.L.Goodman, submitted for publication.
3. J.Krumlinde and Z.Szymanski, Ann. Phys. 79 (1973) 201.
4. S.Bose, J.Krumlinde and E.R.Marshalek, Phys. Lett. 53B (1974) 136.
5. R.A.Sorensen, Nucl. Phys. A269 (1976) 301.
6. S.Chu, E.Marshalek, P.Ring, J.Krumlinde and J.Rasmussen, Phys. Rev. C12 (1975) 1017.
7. J.Krumlinde and E.Marshalek, Nucl. Phys. A275 (1977) 395.
8. E.Marshalek and A.Goodman, Nucl. Phys. A294 (1978) 92.
9. A.L.Goodman, Phys. Rev. Letts. 42 (1979) 357.
10. A.L.Goodman, Nucl. Phys. A325 (1979) 171.

FIGURE CAPTIONS

Fig. 1. Schematic diagram of energy E versus spin I. The energy splits into thermal and collective components. The temperature is T.

Fig. 2. Single-particle states in the two-level model.

Fig. 3. The pair gap Δ versus the temperature in the non-rotating ($\omega = 0$) case.

Fig. 4. The pair gap Δ versus the angular velocity ω for various temperatures. The quantities Δ, ω, kT, G and ε have units of MeV. The critical temperature kT_c is 0.498 MeV.

Fig. 5. See Fig. 4. The critical temperature kT_c is 0.485 MeV.

Fig. 6. The critical spin I_c versus the temperature.

Fig. 7. The spin I versus the angular velocity ω for various temperatures.

Fig. 8. The moment-of-inertia $\mathcal{J}$ versus the square of the angular velocity ω for various temperatures.

Fig. 9. The internal energy E versus the temperature for various spins.

Fig. 10. The internal energy E versus the spin I for various temperatures.

Fig. 11. The quasiparticle occupation probabilities $f_{\pm}$ versus the temperature for various spins.

Fig. 12. The entropy versus the temperature for various spins.

Fig. 13. The square of the fluctuation in J_x versus the spin for various temperatures.

Fig. 14. The angular momentum fluctuation energy versus the spin for various temperatures.

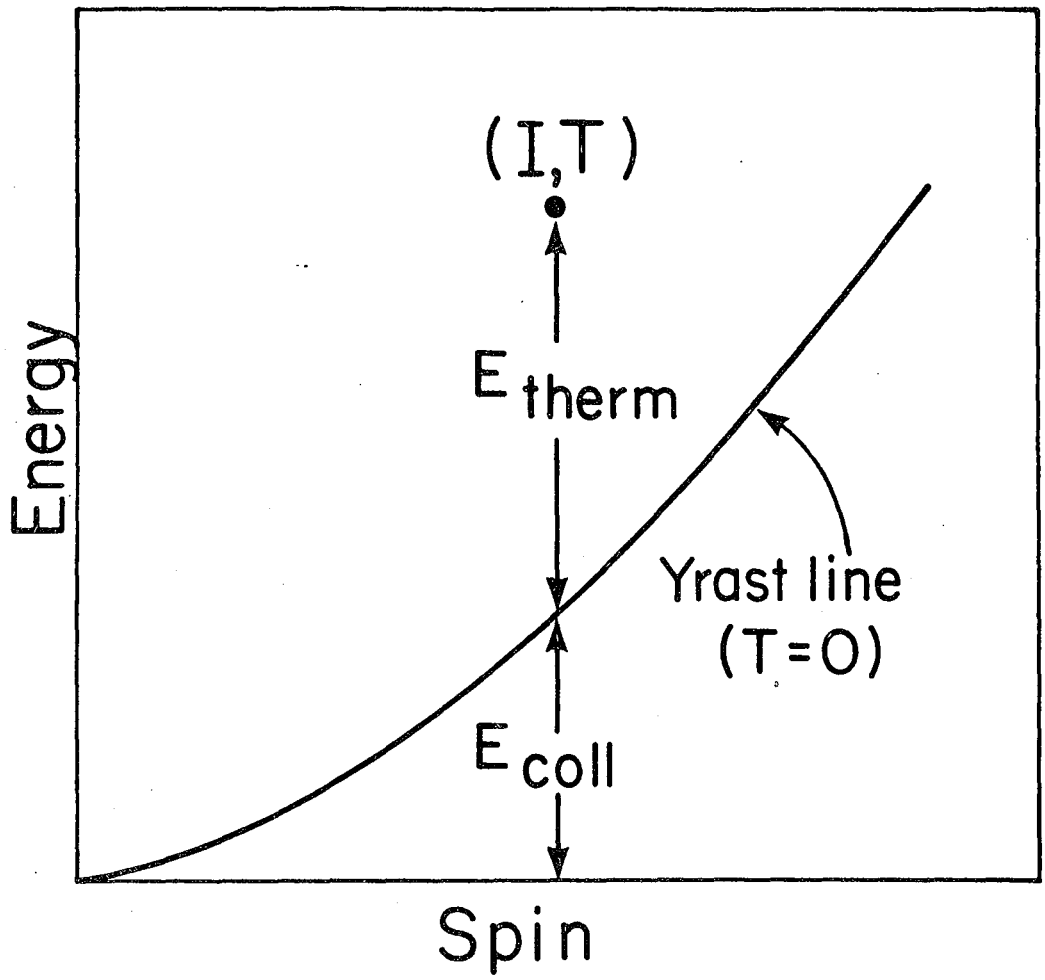

XBL 807-1508

Fig. 1

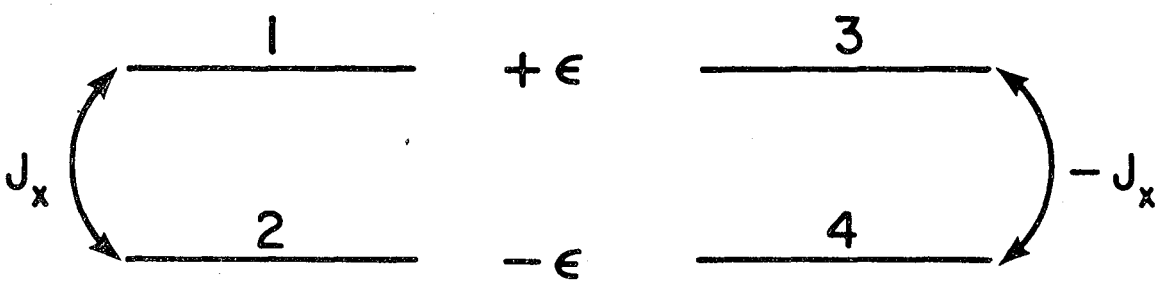

XBL 807-1509

Fig. 2

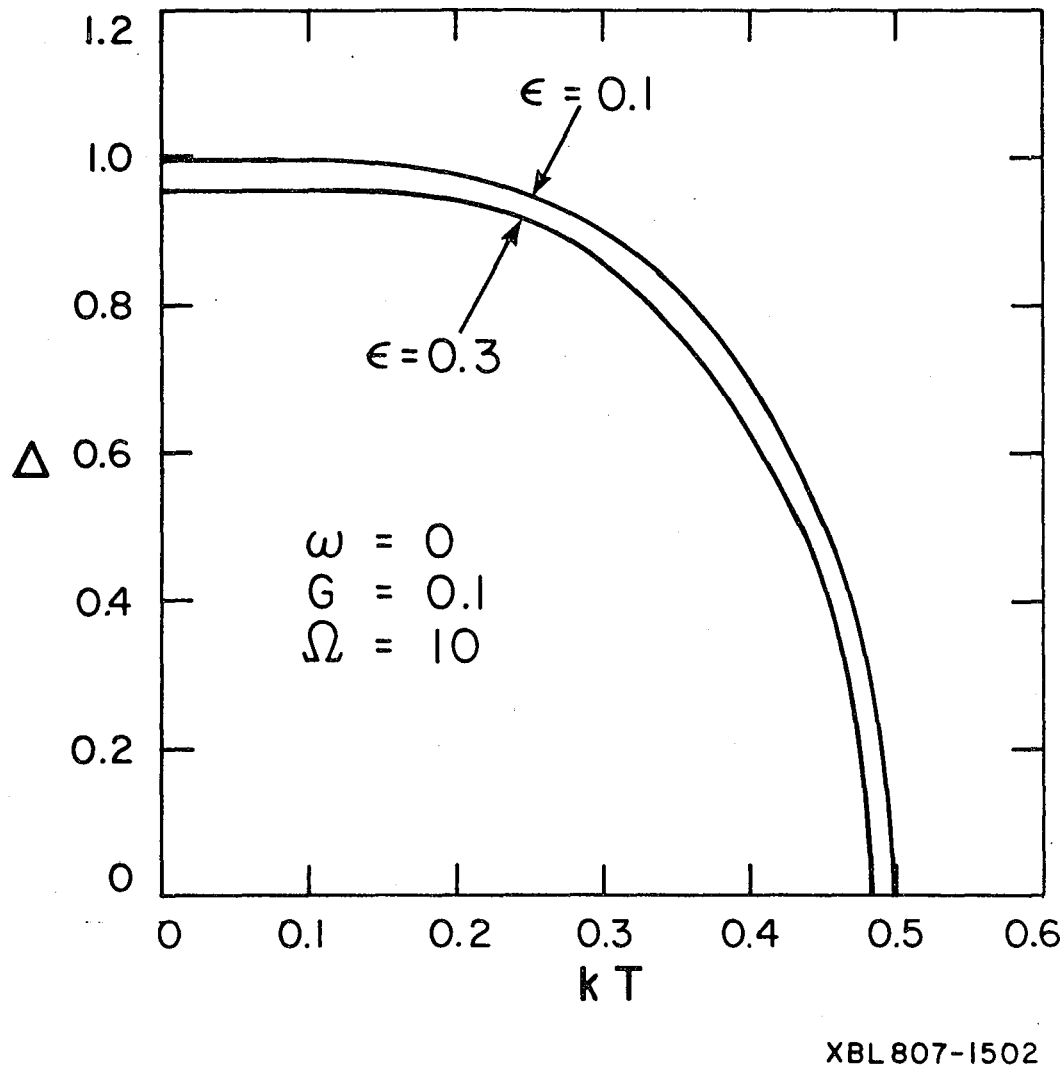
1.2
1.0
0.8
0.6
0.4
0.2
0
Δ
ϵ = 0.1
ϵ = 0.3
ω = 0
G = 0.1
Ω = 10
0
0.1
0.2
0.3
0.4
0.5
0.6
k T
XBL 807-1502

Fig. 3

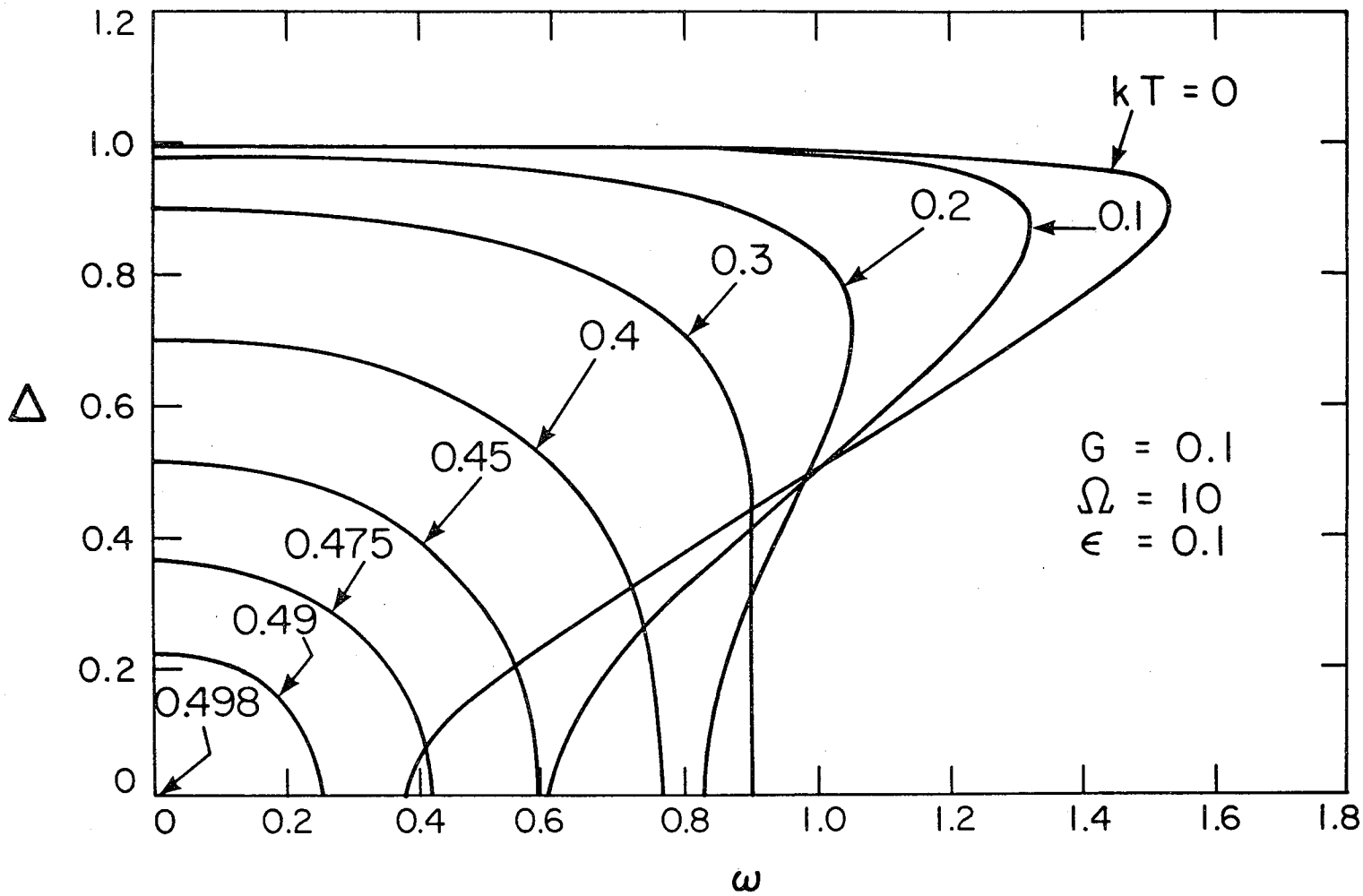

XBL807-1515

Fig. 4

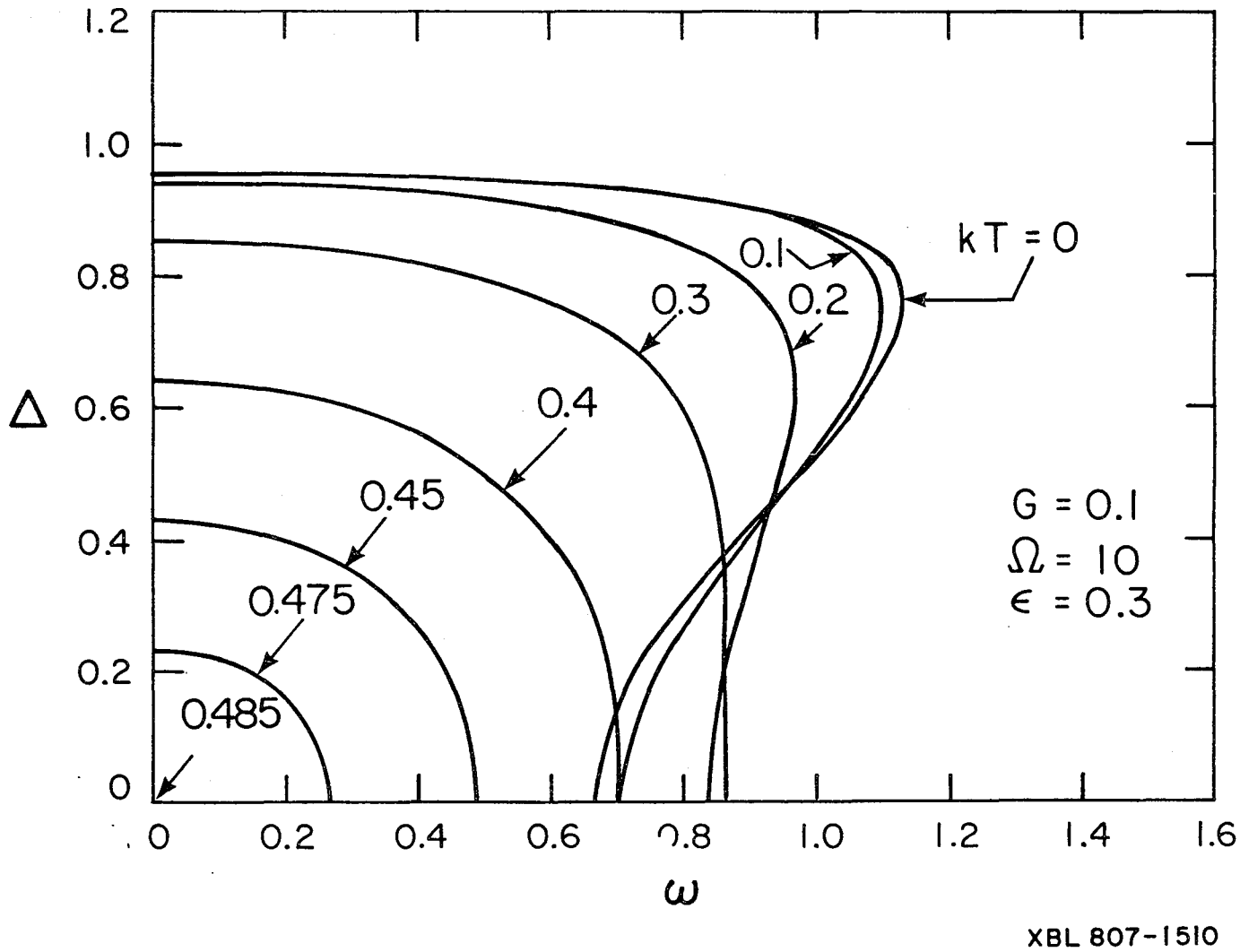

XBL 807-1510

Fig. 5

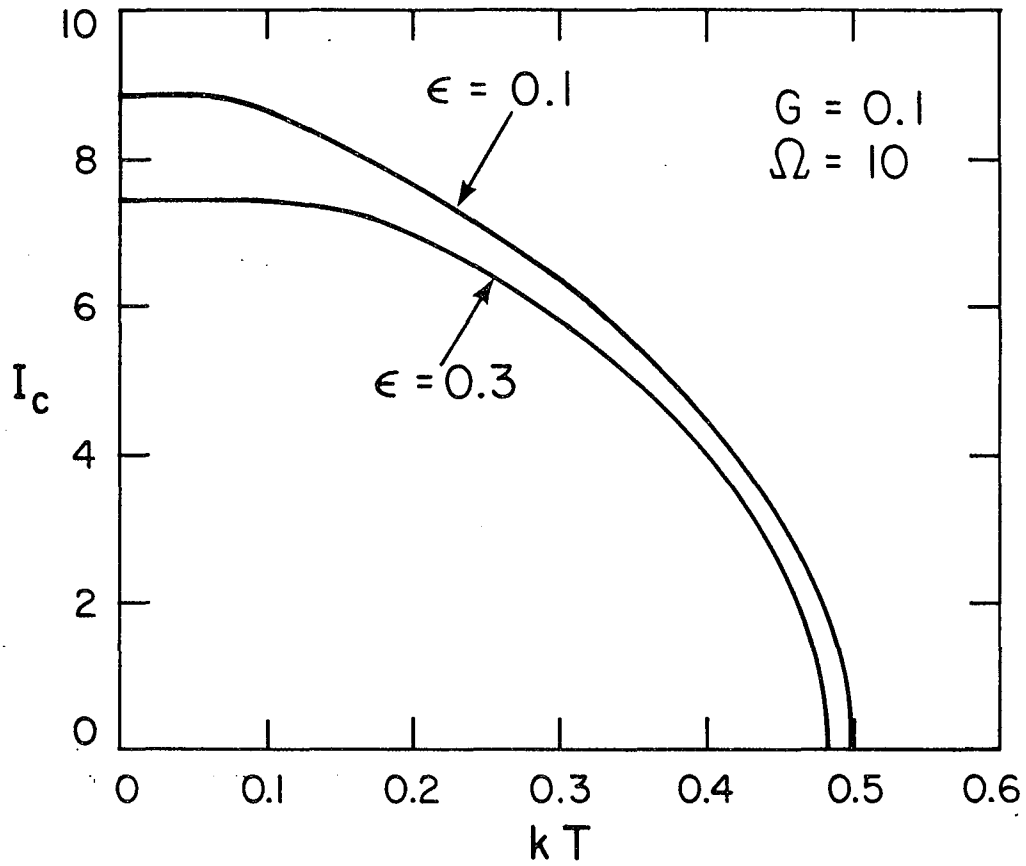

XBL807-1503

Fig. 6

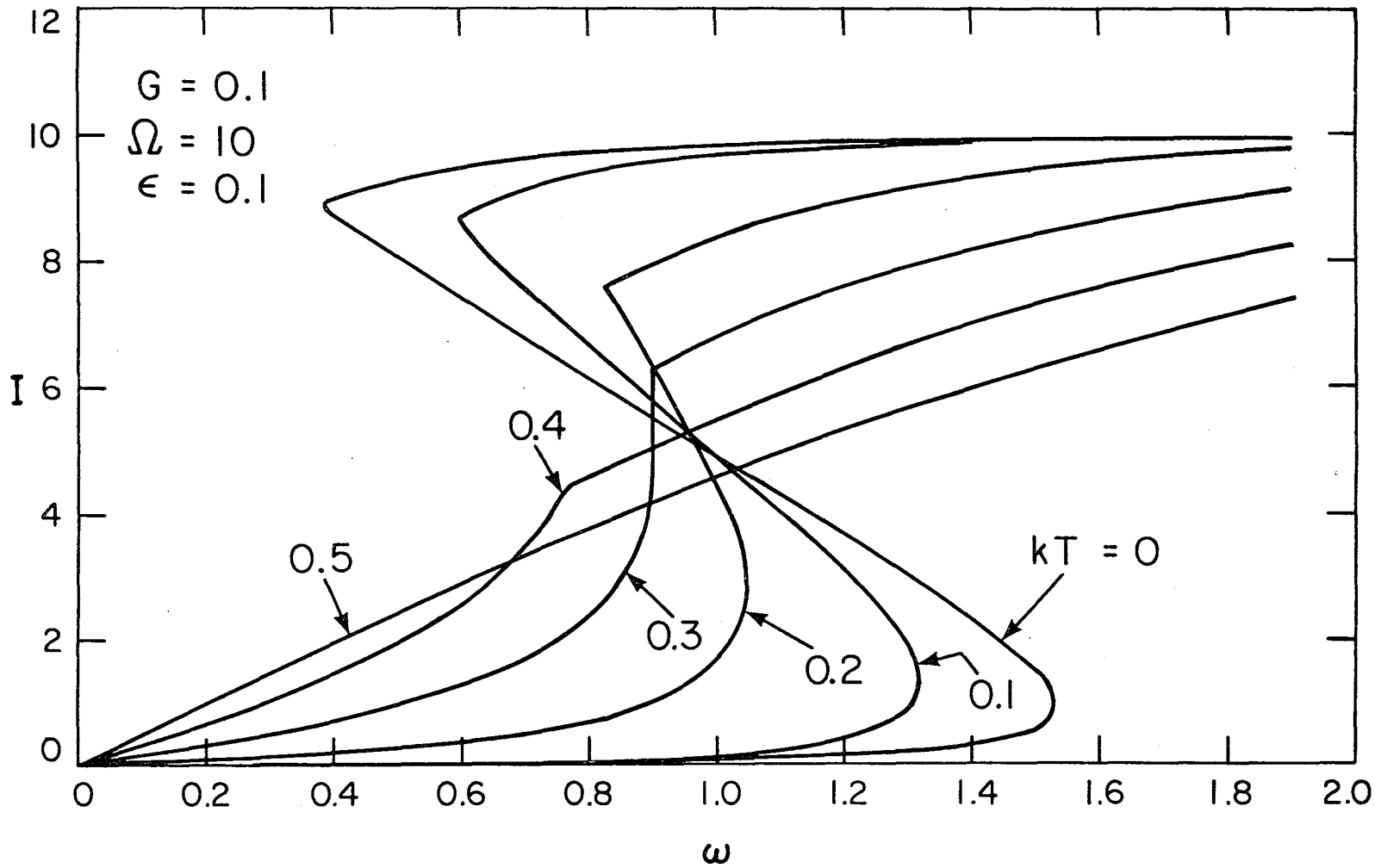

XBL807-1514

Fig. 7

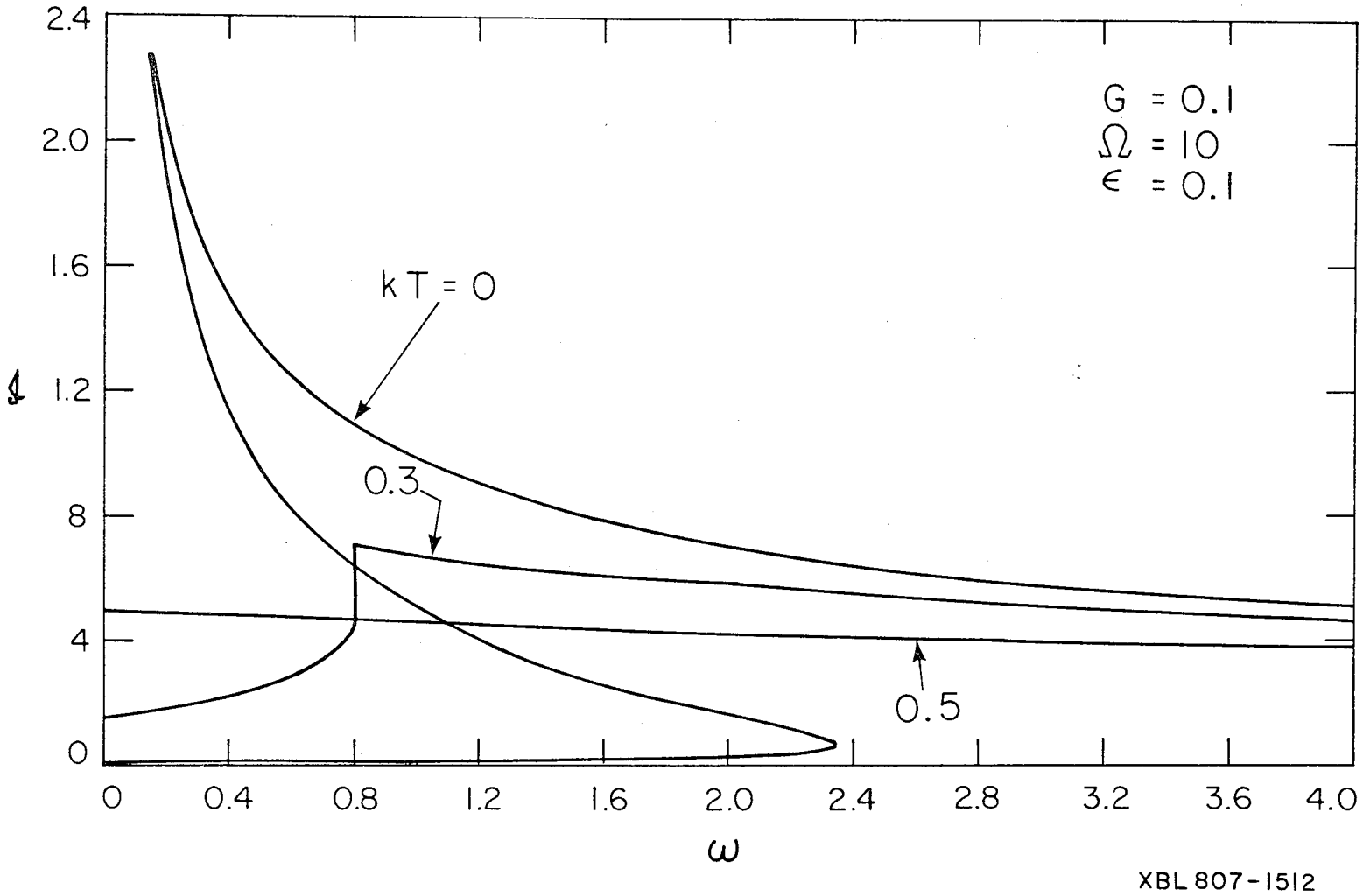
G = 0.1
Ω = 10
ϵ = 0.1
kT = 0
0.3
0.5
2.4
2.0
1.6
1.2
8
4
0
0
0.4
0.8
1.2
1.6
2.0
2.4
2.8
3.2
3.6
4.0
ω
XBL 807-1512

Fig. 8

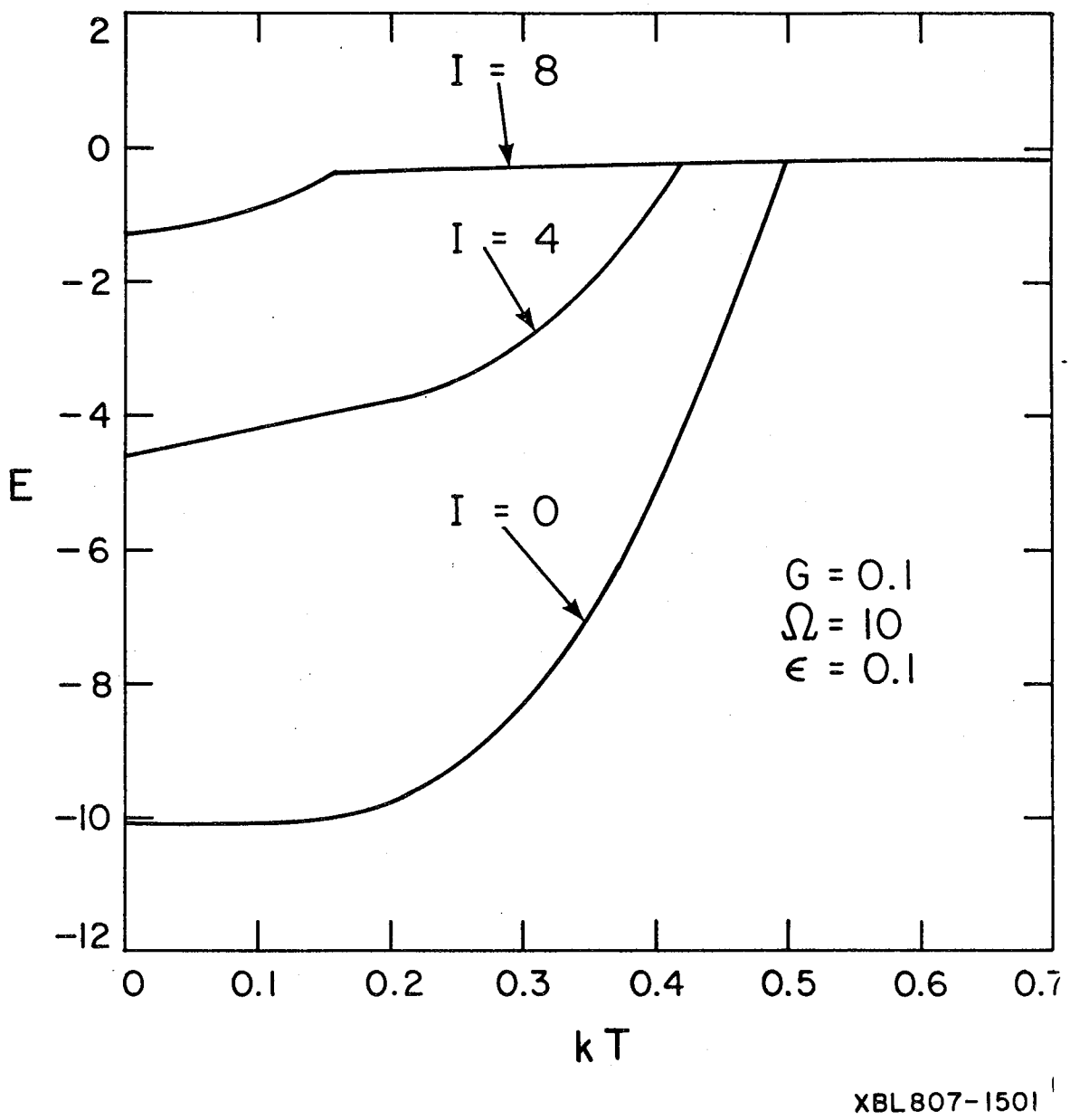
2
0
-2
-4
-6
-8
-10
-12
E
I = 8
I = 4
I = 0
G = 0.1
Ω = 10
ϵ = 0.1
0
0.1
0.2
0.3
0.4
0.5
0.6
0.7
kT
XBL807-1501

Fig. 9

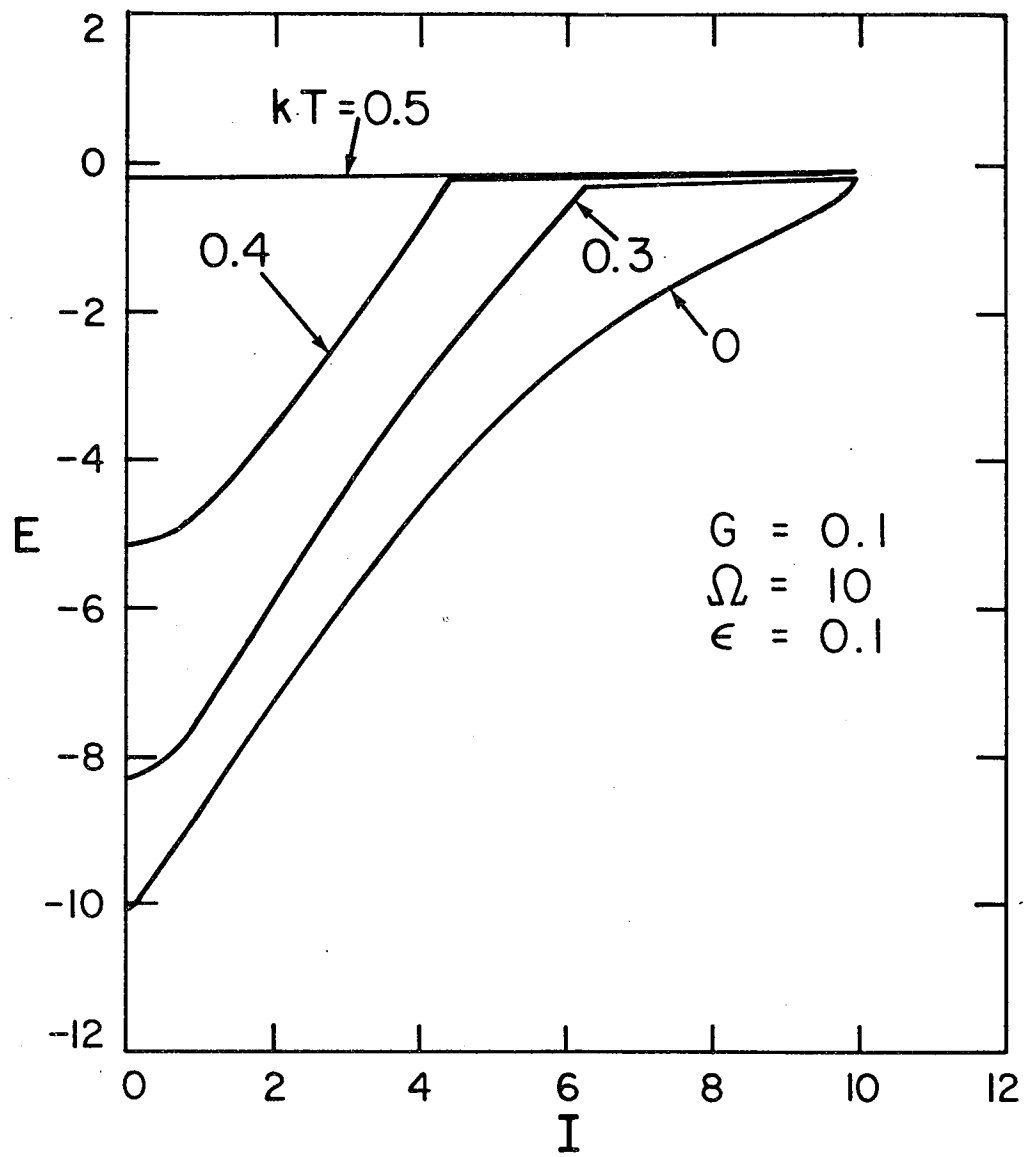

XBL 807-1507

Fig. 10

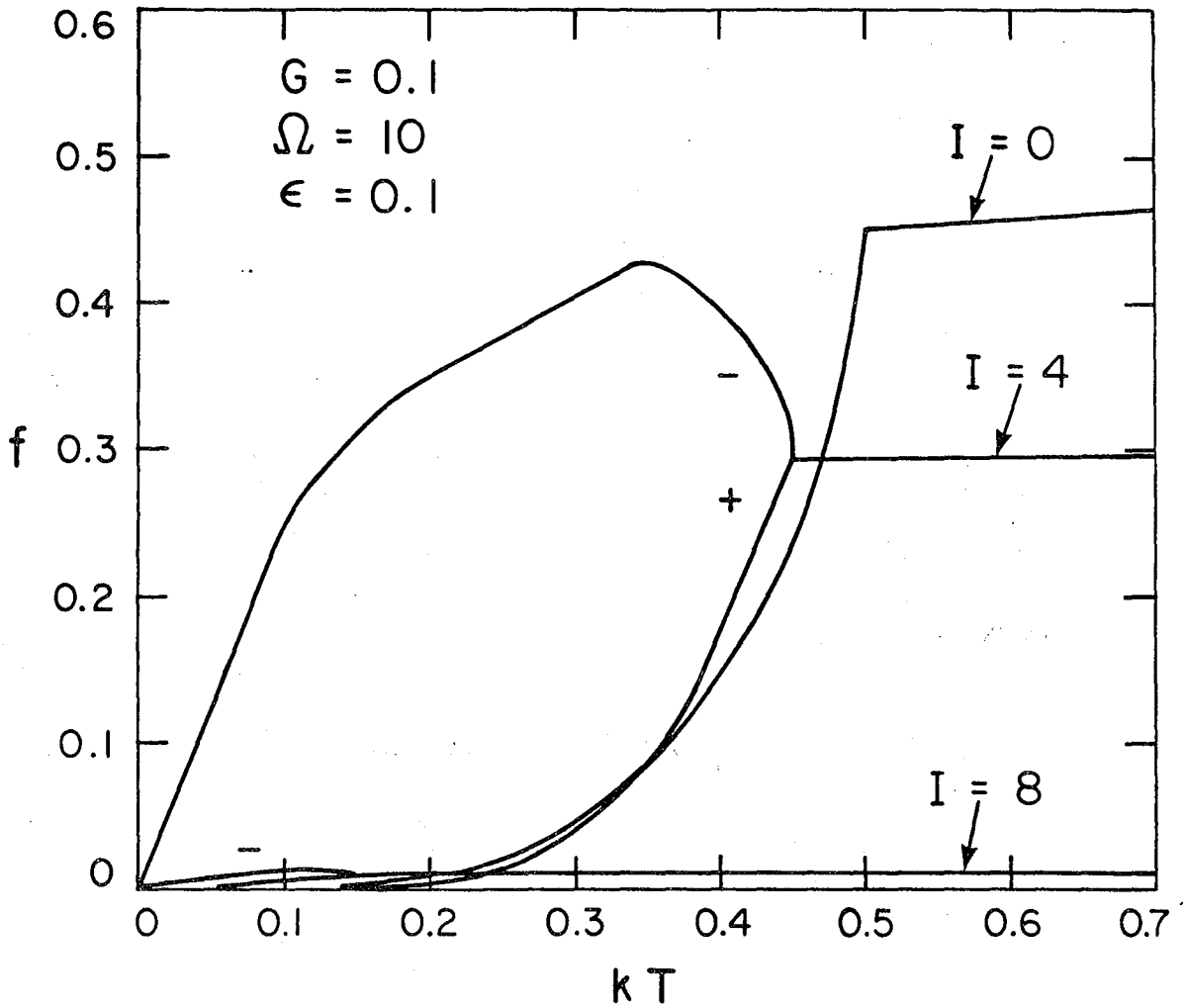

XBL 807-1506

Fig. 11

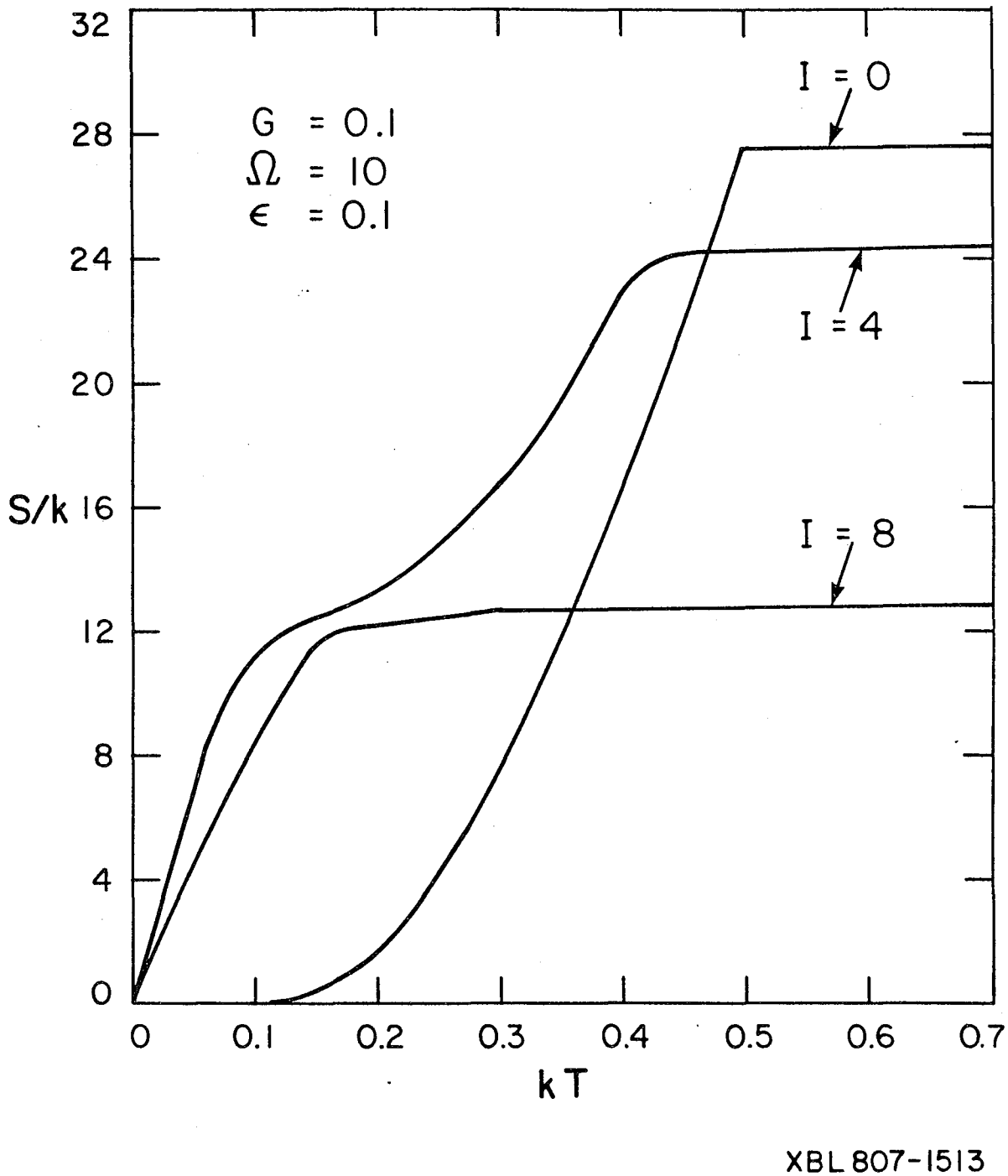

XBL 807-1513

Fig. 12

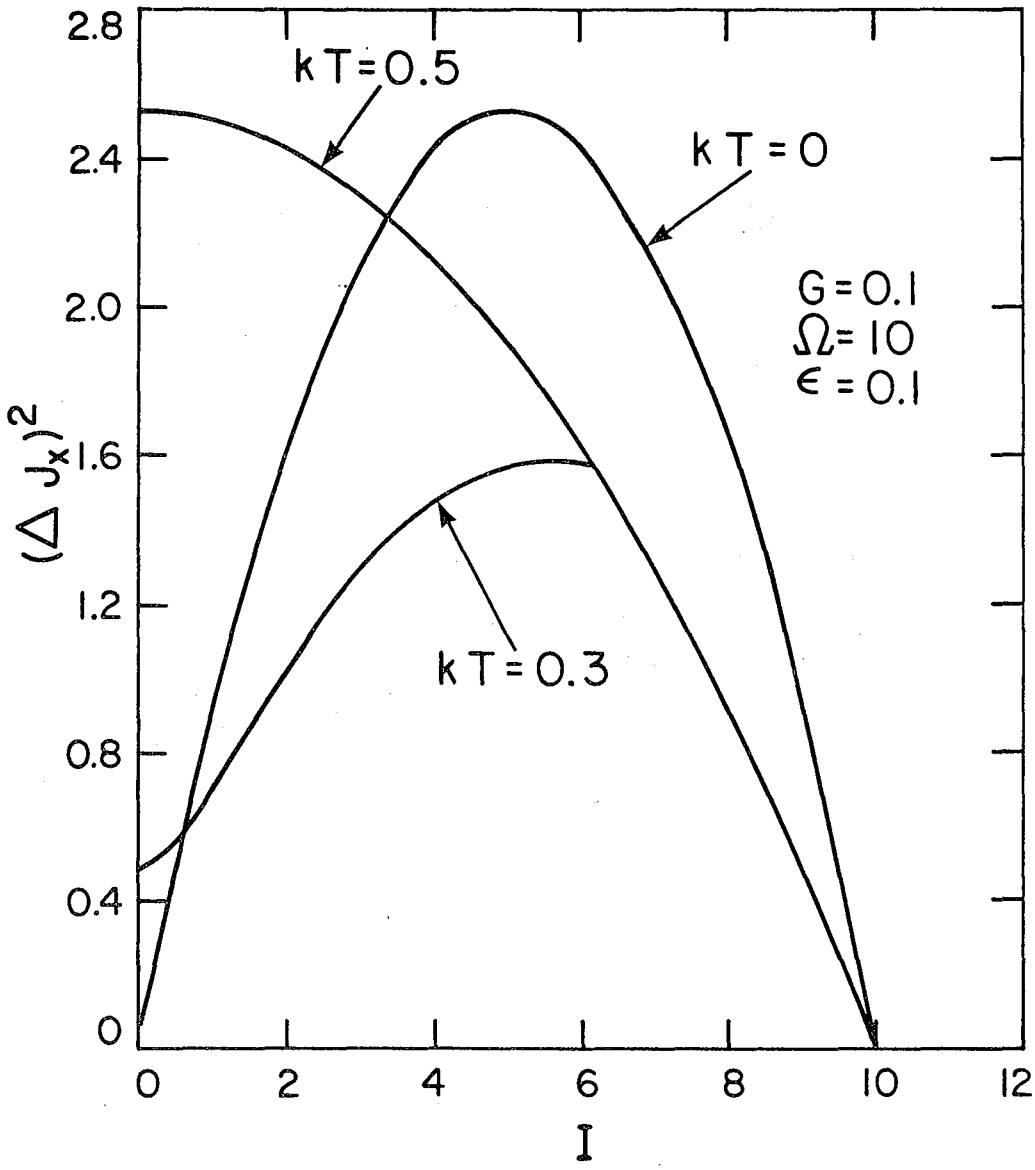

XBL807-1504

Fig. 13

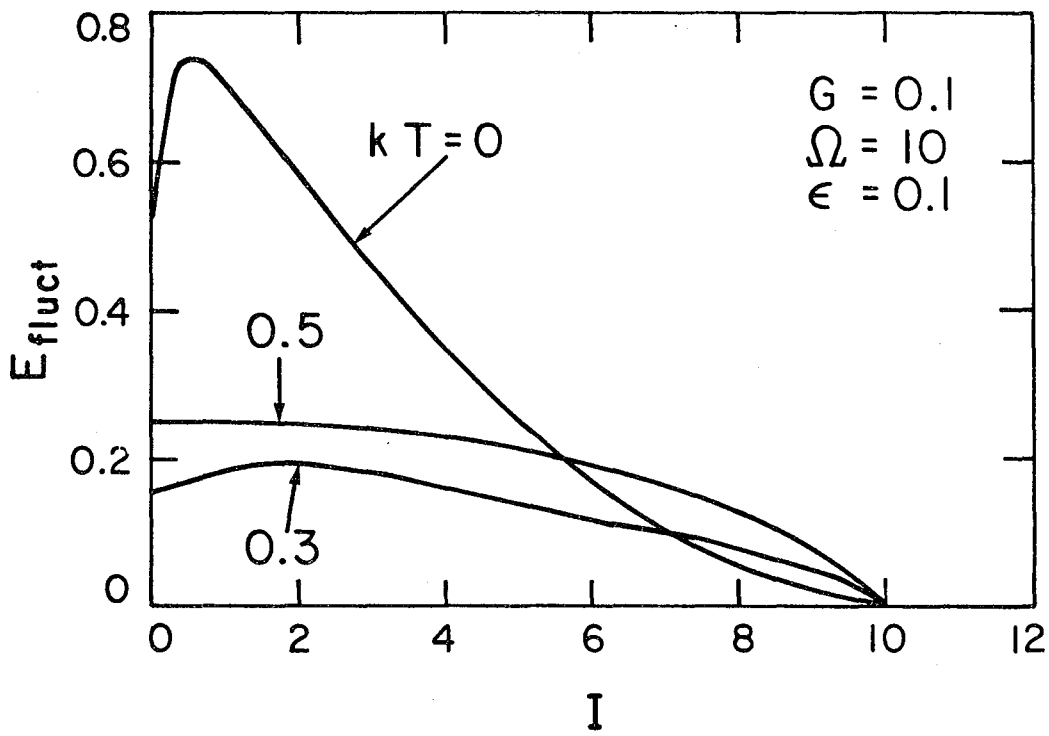

XBL 807-1505

Fig. 14

This report was done with support from the United States Energy Research and Development Administration. Any conclusions or opinions expressed in this report represent solely those of the author(s) and not necessarily those of The Regents of the University of California, the Lawrence Berkeley Laboratory or the United States Energy Research and Development Administration.

0 0 0 0 4 5 0 2 2 9 4